Environmental Tobacco Smoke Effects on the Primary Lipids of Lung Surfactant

Frank Bringezu,[†,‡] Kent E. Pinkerton,[§] and Joseph A. Zasadzinski*[,†]

Department of Chemical Engineering, University of California, Santa Barbara, California 93106-5080, and Department of Anatomy, Physiology and Cell Biology, School of Veterinary Medicine, University of California, Davis, California 95616

Received August 22, 2002. In Final Form: December 2, 2002

The effects of environmental tobacco smoke (ETS) on lung surfactant are difficult to determine from analysis of human and animal lung lavage due to large variations in surfactant recovery, a lack of uniformity of smoke exposure, and the difficulties inherent in analyzing milligram quantities of a multicomponent biological material. An alternative is to examine specific components of lung surfactant in a Langmuir trough with a subphase conditioned by exposure to known quantities of ETS. Pressure−area isotherms and fluorescence microscopy measurements reveal that both the minimum surface tension and respreading of model lung surfactant monolayers and the morphology of the condensed phases at high lateral pressures are changed on subphases exposed to ETS. ETS alters the distribution and fraction of crystalline lipid domains in the monolayer, which are correlated with the minimum surface tension and monolayer viscosity in pristine lung surfactant monolayers. The minimum surface tension of the dominant lipid species in lung surfactant monolayers steadily increases with increased ETS exposure, and surfactant respreading on monolayer expansion is inhibited, which may lead to an increased work of breathing and an altered distribution of alveolar fluids.

Introduction

Tobacco smoke is typically divided into two classes—mainstream smoke, which the smoker inhales, and environmental tobacco smoke (ETS), which primarily comes off the smoldering end of the cigarette or cigar, and which is taken in by others.[1] This so-called "passive smoking" has been identified as a major source of morbidity in the United States.[2,3] The origin of the negative health effects of exposure to ETS, especially among children, who seem to be particularly susceptible,[4−9] is not well understood. There are strong epidemiological correlations between long-term exposure to ETS and lung cancer[5,6] in never-smoking adults. Childhood and/or continuing exposure to ETS is correlated with asthma and/or wheezing and increased respiratory illness in children.[4,7,8] However, recognizing the negative effects of ETS in large populations does not explain the origin of these effects in individuals. Making rational decisions regarding interventions to control or reverse these effects requires a better understanding of the effects of ETS on the lungs.

The mechanisms of injury due to ETS are likely very complex. However, inhaled ETS and other pollutants must first interact with the liquids lining the lung. In the upper airways, this layer is thick and contains high levels of antioxidants. It is likely, therefore, that damage due to ETS is more common in the lower airways and alveoli where the liquid lining the epithelium is thin and contains fewer antioxidants.[10] In this liquid, oxidants, free radicals, and other components of ETS can react with antioxidants or biomolecules, resulting in the inactivation of the biomolecules, or in the formation of even more reactive agents.

In the alveoli and lower airways, the liquid−air interface is coated with a molecular layer of lung surfactant.[11] Lung surfactant is a complex, multicomponent, lipid−protein mixture[11,12] that lowers the surface tension of the interface and minimizes the work associated with expanding and contracting these interfaces during breathing. The primary lipid species in lung surfactants are saturated dipalmitoylphosphatidylcholine (DPPC) and unsaturated phosphatidylcholines and phophatidylglycerols (PGs). In clinically used replacement surfactants such as Survanta and Exosurf, palmitic acid (PA) or hexadecanol is added to enhance performance.[13] Lipids make up 90% of the mass of native surfactant, with the remainder being the lung surfactant-specific proteins SP-A, SP-B, SP-C, and SP-D.[12,14] A lack of effective surfactant, due to either immaturity in premature infants or various diseases in adults, can result in respiratory distress syndrome (RDS).[11,15]

* To whom correspondence should be addressed. E-mail: Gorilla@engineering.ucsb.edu. Phone: (805) 893-4769. Fax: (805) 893-4731.
† University of California, Santa Barbara.
‡ Current Address: Institüt für Medicalische Physik und Biophysik, Liebigstrasse 27, 04103 Leipzig, Germany.
§ University of California, Davis.

(1) Teague, S. V.; Pinkerton, K. E.; Goldsmith, M.; Gebremichael, A.; Chang, S.; Jenkins, R. A.; Moneyhun, J. H. *J. Inhalation Toxicol.* **1994**, *6*, 79−93.
(2) Bartecchi, C. E.; MacKenzie, T. D.; Schrier, R. W. *N. Engl. J. Med.* **1994**, *330*, 907−912.
(3) Bartecchi, C. E.; MacKenzie, T. D.; Schrier, R. W. *N. Engl. J. Med.* **1994**, *330*, 975−980.
(4) Bousquet, J.; Vignola, A. M. *Allergy* **2001**, *56*, 466−469.
(5) Adlkofer, F. *Int. Arch. Occup. Environ. Health* **2001**, *74*, 231−241.
(6) Johnson, K. C.; Hu, J.; Mao, Y. *Int. J. Cancer* **2001**, *93*, 902−906.
(7) Gilliand, F. D.; Li, Y. F.; Peters, J. M. *Am. J. Respir. Crit. Care Med.* **2001**, *163*, 429−436.
(8) Larsson, M. L.; Frisk, M.; Hallstrom, J.; Kiviloog, J.; Lundback, B. *Chest* **2001**, *120*, 711−717.
(9) Lam, T. H.; Leung, G. M.; Ho, L. M. *Pediatrics* **2001**, *107*, E91.
(10) Putman, E.; van Golde, L. M. G.; Haagsman, H. P. *Lung* **1997**, *175*, 75−103.
(11) Notter, R. H. *Lung Surfactants: Basic Science and Clinical Applications*; Marcel Dekker: New York, 2000; Vol. 149.
(12) Goerke, J. *Biochim. Biophys. Acta* **1998**, *1408*, 79−89.
(13) Bernhard, W.; Mottaghian, J.; Gebert, A.; Rau, G. A.; von der Hardt, H.; Poets, C. F. *Am. J. Crit. Care Med.* **2000**, *162*, 1524−1533.
(14) Possmayer, F. *Am. Rev. Respir. Dis.* **1988**, *138*, 990−998.
(15) Clements, J. A. *Physiologist* **1962**, *5*, 11−28.

10.1021/la026455e CCC: $25.00
Published on Web 02/20/2003

Oxidation or other reactions of surfactant constituents may alter the composition and morphology of surfactant monolayers essential to good surfactant performance.[16−19] Recent studies have confirmed oxidative[10,17] and/or free radical damage[16] to the surfactant can result in higher minimum surface tensions and poor performance. It would not be surprising to find that the constituents of ETS, which is known to contain both free radicals and strong oxidizers, might chemically or physically alter lung surfactant and impair surfactant function.[1] Our work on surfactants on smoke-free subphases has shown that relatively small variations in surfactant protein[18,20−22] or lipid composition[22−26] can lead to large changes in surfactant performance. Hence, it is not surprising that the oxidizing and free radical compounds found in ETS[1,27,28] should lead to surfactant damage and poor surfactant performance. In vivo studies have also shown that many of the components present in tobacco smoke and other environmental pollutants can react with the components of lung surfactant,[10,17,29−37] and that the antioxidant properties of the lung change in response to smoking.[38]

Previous attempts to elucidate the effects of mainstream smoke have typically involved rinsing either rodent[38−41] or human[30,42,43] lungs with saline—a technique known as bronchoalveolar lavage (BAL)—and then separating the surfactant from other materials to obtain samples of lung surfactant from nonsmoking controls and rats with varied mainstream smoke exposure. Some studies suggest that the total amount of phospholipids in BAL is reduced,[29,30,35,39,43] perhaps due to a smoke-induced decrease in secretion from the alveolar type II cell.[44] Other studies find little change in the total phospholipid content, but rather alterations in the relative fractions of phosphatidylcholine, sphingomyelin, or phosphatidylethanolamine,[42] the relative fractions of saturated vs unsaturated lipids,[40] or the relative amounts of lung surfactant-specific protein SP-B or SP-A.[41] Few studies examine the effects of these changes in lung surfactant composition or quantity on the surface properties of lung surfactant.[40,45] Higenbottom[45] showed that exposure to tobacco smoke induced substantial changes to the normal expansion and compression isotherms of bovine surfactant. Subramaniam et al. showed that the compressibility and respreading of lung surfactant extracted from BAL of smoke-exposed rats was inferior to that of controls,[40] and correlated this with a decrease in the saturated phosphatidylcholine fraction of the smoke-exposed rat surfactant. However, due to the rather large variability in the extraction, separation, and analysis of BAL even in control animals, it is difficult to reach a consensus on the effects of mainstream smoke on lung surfactant quantity or quality.

To begin to isolate the physical and chemical changes in lung surfactant on exposure to ETS requires a simplified model surfactant lipid mixture and a controlled ETS-exposure method. Our in vitro model of the epithelial lining liquids of the lungs is a Langmuir trough, filled with an aqueous "subphase", onto which monolayers of the lipids corresponding to lung surfactants are spread.[12,15] The subphase on which the model lung surfactants are spread is conditioned by exposure to known concentrations of ETS from a smoking machine[44] that correspond to realistic exposure levels.[1] Such lipid monolayers at the air−water interface provide excellent model systems for the study of the organization and function of lung surfactants.[15,20,21] Care is necessary to extrapolate model monolayer behavior in vitro to lung surfactant behavior in vivo, but general correlations are starting to emerge.[12,18,21,46]

The variation of surface tension with monolayer area of the surfactant lipids is determined by surface pressure−area isotherms (Figures 1−3). The morphology of the monolayer domains is accessible by fluorescence microscopy[47] (Figures 4−6). The combination of these methods gives a detailed view of the relationship between monolayer organization and composition and low minimum surface tension and rapid respreading. Our isotherm and fluorescence microscopy results show that ETS alters the distribution and fraction of crystalline lipid domains in the monolayer, which are correlated with the minimum surface tension at monolayer collapse,[11,12,18,21,23,48,49] respreading of the surfactant on expansion of the interface,[11,21,23,46,48−51] and monolayer viscosity[26] in pristine lung surfactant monolayers. The minimum surface tension

(16) Mark, L.; Ingenito, E. P. *Am. J. Physiol.* **1999**, *276*, L491−500.
(17) Andersson, S.; Kheiter, A.; Merritt, T. A. *Lung* **1999**, *177*, 179−189.
(18) Ding, J.; Takamoto, D.; von Nahmen, A.; Lipp, M. M.; Lee, K. Y. C.; Waring, A. J.; Zasadzinski, J. A. *Biophys. J.* **2001**, *80*, 2262−2272.
(19) Warriner, H. E.; Ding, J.; Waring, A.; Zasadzinski, J. A. *Biophys. J.* **2002**, *82*, 835−842.
(20) Lipp, M. M.; Lee, K. Y. C.; Zasadzinski, J. A.; Waring, A. J. *Science* **1996**, *273*, 1196−1199.
(21) Lipp, M. M.; Lee, K. Y. C.; Takamoto, D. Y.; Zasadzinski, J. A.; Waring, A. J. *Phys. Rev. Lett.* **1998**, *81*, 1650−1653.
(22) Takamoto, D. Y.; Lipp, M. M.; von Nahmen, A.; Lee, K. Y. C.; Waring, A. J.; Zasadzinski, J. A. *Biophys. J.* **2001**, *81*, 153−169.
(23) Bringezu, F.; Ding, J.; Brezesinski, G.; Zasadsinksi, J. A. *Langmuir* **2001**, *17*, 4641−4648.
(24) Bringezu, F.; Ding, J.; Brezesinski, G.; Waring, A.; Zasadzinski, J. A. *Langmuir*, in press.
(25) Ding, J.; Warriner, H. E.; Zasadzinski. *Langmuir* **2002**, *18*, 2800−2806.
(26) Ding, J.; Warriner, H. E.; Zasadzinski, J. A. *Phys. Rev. Lett.*, in press.
(27) Douce, D. S.; Clench, M. R.; Frost, B. *J. Environ. Monit.* **2001**, *3*, 295−301.
(28) Nelson, P. R.; Conrad, F. W.; Kelly, S. P.; Maiolo, K. C.; Richardson, J. D.; Ogden, M. W. *Environ. Int.* **1998**, *24*, 251−257.
(29) Lusuardi, M.; Capelli, A.; Carli, S.; Tacconi, M. T.; Salmona, M.; Donner, C. F. *Respiration* **1992**, *59*, 28−32.
(30) Schmekel, B.; Khan, A. R.; Linden, M.; Wollmer, P. *Clin. Physiol.* **1991**, *11*, 431−438.
(31) Jablonka, S.; Ledwozyw, A.; Kadziolka, W.; Modrzewski, Z. *Pneumonol. Pol.* **1989**, *57*, 270−276.
(32) Higenbottam, T. *Respiration* **1989**, *55*, 14−27.
(33) Todisco, T.; Dottorini, M.; Rossi, F.; Baldonici, A.; Palumbo, R. *Respiration* **1989**, *55*, 84−93.
(34) Giamonna, S. T.; Tocci, P.; Webb, W. R. *Am. Rev. Respir. Dis.* **1971**, *104*, 358−367.
(35) Finley, T.; Ladman, A. *N. Engl. J. Med.* **1972**, *286*, 223−227.
(36) Postlethwait, E. M.; LAngford, S. D.; Jacobson, L. M.; Bidani, A. *Free Radical Biol. Med.* **1995**, *19*, 553−563.
(37) Pegnatelli, B.; Li, C. Q.; Boffetta, P.; Chen, Q.; Ahrens, W.; Nyberg, F.; Mukeria, A.; Bruske-Hohlfeld, I.; Fortes, C.; Constantinescu, V.; Ischiropoulos, H.; Ohshima, H. *Cancer Res.* **2001**, *61*, 778−784.
(38) Wurzel, H.; Yeh, C. C.; Gairola, C.; Chow, C. K. *J. Biochem. Toxicol.* **1995**, *10*, 11−17.
(39) Le Mesurier, S. M.; Stewart, B. W.; Lykke, A. W. *Environ. Res.* **1981**, *24*, 207−217.
(40) Subramaniam, S.; Bummer, P.; Gairola, C. G. *Fundam. Appl. Toxicol.* **1995**, *27*, 63−69.
(41) Subramaniam, S.; Whitsett, J. A.; Hull, W.; Gairola, C. G. *Toxicol. Appl. Pharmacol.* **1996**, *140*, 274−280.
(42) Mancini, N. M.; Bene, M. C.; Gerard, H.; Chabot, F.; Faure, G.; Polu, J. M.; Lesur, O. *Lung* **1993**, *171*, 277−291.
(43) Zetterberg, G.; Curstedt, T.; Eklund, A. *Sarcoidosis* **1995**, *12*, 46−50.
(44) Wirtz, H. R. W.; Schmidt, M. *Eur. Respir. J.* **1996**, *9*, 24−32.
(45) Higenbottam, T. *Tokai J. Exp. Clin. Med.* **1985**, *10*, 465−470.
(46) Schürch, S.; Green, F. H. Y.; Bachofen, H. *Biochim. Biophys. Acta* **1998**, *1408*, 180−202.
(47) McConnell, H. *Anny. Rev. Phys. Chem.* **1991**, *42*, 171−195.
(48) Bangham, A.; Morley, C.; Phillips, M. *Biochim. Biophys. Acta* **1979**, *573*, 552−556.
(49) Lee, K. Y. C.; Gopal, A.; von Nahmen, A.; Zasadzinski, J. A.; Majewski, J.; Smith, S.; Howes, P. B.; Kjaer, K. *J. Chem. Phys.* **2002**, *116*, 774−783.
(50) Pison, U.; Herold, R.; Schürch, S. *Colloids Surf.* **1996**, *114*, 165−184.
(51) Veldhuizen, R.; Nag, K.; Orgeig, S.; Possmayer, F. *Biochim. Biophys. Acta* **1998**, *1408*, 90−108.

of monolayers of the dominant lipid species in lung surfactant exposed to ETS steadily increases in vitro, which is correlated with an increased work of breathing and an altered distribution of alveolar fluids in vivo.[11] The effects of ETS on the model lung surfactant lipids are similar to those determined by Subramaniam et al.[40] in surfactant extracted from rat BAL after mainstream smoke exposure, suggesting that ETS has effects similar to those of mainstream smoke on surfactant function. These physical and chemical alterations of lung surfactant help explain the mechanism by which ETS degrades the function of lung surfactant. Of course, only those components of ETS that are soluble in the subphase water can interact with the surfactant in our model system; hence, we are probably underestimating the actual effects of ETS on the surfactant. Even so, the increased minimum surface tension and poor respreading we see may promote inflammation and edema, further impairing the surfactant system,[10] perhaps leading to the negative health consequences seen in epidemiological studies of children.[4−9]

Experimental Section

Materials. Disaturated 1,2-dipalmitoyl-*sn*-glycero-3-phosphatidylcholine (DPPC) and mono-unsaturated 1-palmitoyl-2-oleyl-*sn*-glycero-3-phosphatidylglycerol (POPG) were purchased from Avanti Polar Lipids (Alabaster, AL; purity >99%). Palmitic acid (PA) was from Sigma Chemical Co. (St. Louis, MO; purity >99%). Water was prepared using a Millipore Milli-Q system and had a resistivity >18 MΩ cm^{-1}.

Preparation of the ETS-Conditioned Subphases. The smoke exposure system used in this study has been described elsewhere.[1] ETS was generated by burning temperature- and humidity-conditioned 1R4F reference cigarettes (Tobacco and Health Research Institute, University of Kentucky, Lexington, KY) in a smoking machine. Each cigarette was smoked under rigid conditions of 1 puff (35 mL for 2 s)/min for 8 min. A mixture of 89% sidestream smoke and 11% mainstream smoke was collected from the cigarettes in a dilution chimney and drawn into a glass and stainless steel conditioning chamber to be aged and diluted with filtered air for a mean resident time of 2 min. A portion of the air and smoke from the conditioning chamber was further mixed with fresh filtered air before entering the 0.44 m^3 exposure chambers where the gas stream was exposed to the Millipore water in open Petri dishes for 5.5 h. During the exposure, both the total suspended particulates (average total suspended particulates in the chambers, 137 mg/m^3) and the nicotine concentration in air (15 mg/m^3) were measured. After exposure, the stock solution had a pH of 9, a surface tension of 68 ± 1 mN/m, and a nicotine concentration of 0.23 mg/mL. Typical total suspended particulate concentrations in smoky rooms range from about 1 to 4 mg/m^3, and individual exposure times can vary from hours to days, so the stock solution was diluted to approximate this range of concentrations and exposures for use as a subphase for the monolayer experiments. Concentrations of the diluted stock solutions are listed as the equivalent total suspended particulate concentrations (stock solution exposed at 137 mg/m^3 diluted by a factor of 10 would be a 13.7 mg/m^3 equivalent total suspended particulate exposure). We assumed that diluting the stock solution was equivalent to exposing the subphase to the equivalent particulate level. The pH of the diluted solutions was approximately 7. The stock solution and the diluted subphases were not filtered because Higenbottom[45] showed that water-insoluble particulates can play a dominant role in influencing surfactant behavior. The stock solutions were stored in sealed, glass jars until ready for use.

Methods. The monolayer experiments were performed in a custom-built Langmuir trough equipped with a Wilhelmy-type surface pressure measuring device and two computer-controlled barriers that provide symmetric monolayer compression. Monolayers were spread from a 1 mg/mL mixture of DPPC/POPG/PA (69/20/11 w/w/w) in chloroform as representative of the lipids in lung surfactant; these lipid fractions are consistent with the composition of Survanta, a clinically used replacement lung surfactant.[13] DPPC is representative of the saturated neutral phospholipids, and POPG is representative of the unsaturated, anionic lipids. PA is added to adjust the solid-phase fraction and make the mixture similar to the composition of Survanta, a clinically used, bovine extract replacement surfactant.[13] The lipid solution was spread onto pure water or ETS-exposed subphases to form monolayers at the liquid−air interface after the surface was first carefully aspirated to a near zero surface pressure to minimize the effect of any surface-active components of ETS. The monolayer was allowed to equilibrate on the subphase for about 10 min prior to the first compression to ensure complete removal of any residual spreading solvent. Compression rates were varied from 0.13 to 0.91 $Å^2$ mol^{-1} s^{-1} (compression−expansion cycles ranging from about 4 min to about 30 s), and the temperature was varied from room temperature (23 °C) to physiological temperature (37 °C). Every isotherm was repeated at least five times; the reproducibility was ±3 mN/m in surface pressure and ±5% in molecular area. No significant variation in the maximum/minimum surface pressure, respreading, or morphology was observed with temperature or compression speed.

For imaging the monolayers, a Nikon Optiphot with the stage removed was positioned above the trough, with a 40× power long working distance objective designed for use with fluorescence illumination along with a 100 W high-pressure mercury lamp for excitation. A dichroic mirror/barrier filter assembly was used to direct the excitation light onto the monolayer (with a normal angle of incidence) and to filter the emitted fluorescence. The emitted fluorescence was collected by the objective and detected via a silicon-intensified target (SIT) camera. Images were recorded by a JVC super VHS VCR and digitized via a Scion frame grabber.[18−22] The lipid mixtures were doped with 0.5−1 mol % fluorescent lipid Texas Red-DHPE (Molecular Probes) for fluorescence imaging. The fluorescent dye partitions into the more disordered liquid-expanded domains, and is expelled from the better-ordered liquid-condensed and solid-phase domains. Hence, fluid regions in the monolayer appear bright and more crystalline regions appear dark in the fluorescence images.[47]

To quantify the fluorescence and hence the fraction of fluid lipids, low-resolution survey images (not shown) were processed using IDL version 5.3.1 Win 32 from Research Systems, Inc. (Boulder, CO). IDL reads each image as a 900 × 600 array of pixels with values between 0 and 255; 0 corresponds to black and 255 to white. A histogram of the gray scales was constructed using 26 bins of 10 Gy scales in width (except for the final bin, which had only six levels). The number fraction of pixels with, for example, gray levels between 0 and 9 corresponds to bin one, the number fraction of pixels with gray levels from 10 to 19 is in bin two, etc. Gray levels near zero imply a relative lack of fluorescent dye in the area of the image corresponding to those pixels, while gray levels near 255 correspond to a relatively higher concentration of fluorescent dye in those pixels. An absence of fluorescent dye correlates with an absence of fluid lipid phases in the image.[47]

Results

Figure 1 shows a typical isotherm for the model surfactant lipid mixture on water. The vertical axis is the surface pressure, π, which is the reduction in surface tension relative to that of pure water (the surface tension of water is 72 mN/m at 23 °C). A maximum surface pressure (minimum surface tension), also known as the collapse pressure, near 70 mN/m, is characteristic of a good lung surfactant.[11] The horizontal axis gives the average molecular area per lipid hydrocarbon chain (one per PA and two per DPPC or POPG). At pressures above 40 mN/m, a large, constant slope indicates a low compressibility of the monolayer consistent with a solid-phase monolayer. Monolayer collapse occurs at a high pressure (π_{coll}) of about 67 mN/m. On expanding the collapsed film, the pressure drops immediately to about 20 mN/m, accompanied by a gradual increase in area as the surface pressure drops further, which indicates a respreading of the collapsed material over the interface. After the first compression (which is influenced by how the monolayer

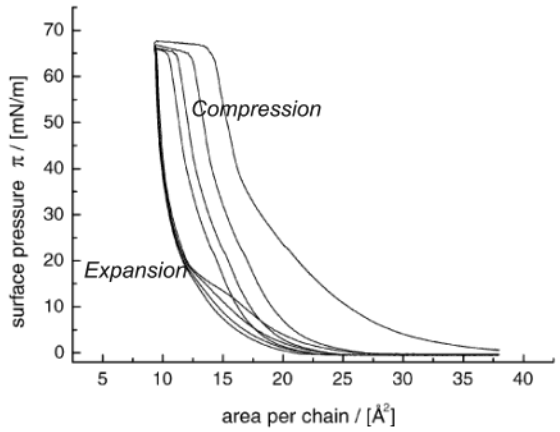

Figure 1. Typical isotherm for the model lung surfactant lipid mixture DPPC/POPG/PA (69/20/11 w/w/w) on water at 23 °C at a quasi-static compression rate of 0.13 Å^2 mol^{-1} s^{-1}. The surface pressure, π, is the reduction in surface tension relative to that of pure water; the horizontal axis gives the average molecular area per lipid hydrocarbon chain (one per PA and two per DPPC or POPG). A sustained maximum surface pressure, also known as the collapse pressure, near 70 mN/m, is characteristic of a good lung surfactant, as is the hysteresis between the compression (right) and expansion (left) parts of the cycle.

is spread from the solvent), the expansion and compression cycles were more reproducible, with a consistent collapse pressure of 65 ± 3 mN/m. This behavior is typical of a good lung surfactant, and the isotherms are similar to those of Survanta under similar conditions.[18]

Figure 2 shows isotherms collected at higher compression speeds and physiological temperature (37 °C) to better mimic physiological conditions. While it is common in the literature to examine quasi-statically compressed lung surfactant monolayers,[15,18,20,21] the compression speed may modify the collapse pressure and the monolayer compressibility.[47] This has been explored somewhat in pulsating and captive bubble techniques that cycle the interfacial area at higher speeds.[11,46] Figure 2A shows the cyclic isotherms obtained at a compression speed of 0.91 Å^2 mol^{-1} s^{-1}, which was the highest speed possible for our trough (an increase of a factor of 7 over our normal compression speed). At this speed, one compression−expansion cycle takes about 30 s (normal respiration takes about 5 s/cycle). At a temperature of 23 °C (Figure 2A), monolayer collapse occurs at a surface pressure of 71 ± 3 mN/m, which is not much different from the 65 ± 3 mN/m at the slower compression speed. After the first cycle (which is influenced by the spreading solvent), the subsequent compression−expansion cycles are reproducible. The cyclic isotherm obtained at 37 °C and a compression speed of 0.91 Å^2 mol^{-1} s^{-1} is shown in Figure 2B. After the first compression, the cycles are reproducible and similar to those in Figure 2A. Although there are qualitative differences between the isotherms, the general behavior of the surfactant monolayer is quite similar at all temperatures (over the range of 20−37 °C) and compression−expansion cycle speeds tested. The main differences are at smaller areas per molecule, which is probably the result of the relatively high viscosity of monolayer films causing a slow relaxation toward a uniform state of compression.[25] If the compression is halted during the higher compression speed isotherm, the surface pressure at a given area per molecule adjusts itself toward that in Figure 1. However, what is most important to evaluating lung surfactant performance is that the maximum and minimum surface pressures and the

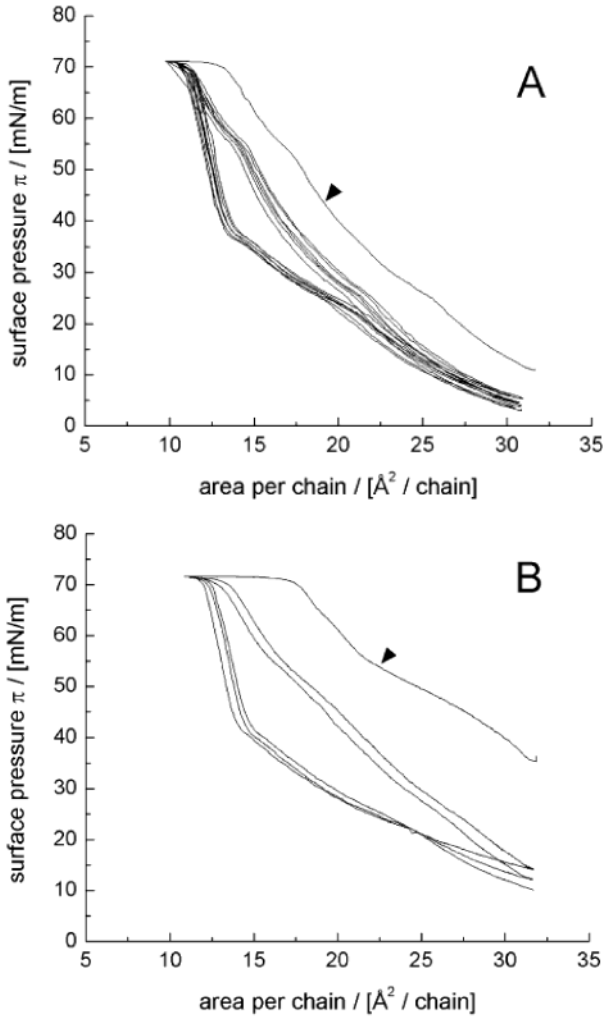

Figure 2. (A) Typical isotherm for the model lung surfactant lipid mixture DPPC/POPG/PA (69/20/11 w/w/w) on water at 23 °C at a compression rate of 0.91 Å^2 mol^{-1} s^{-1} (compression−expansion cycles of about 30 s, about 7 times faster than in Figure 1). The maximum surface pressure was about 71 mN/m, similar to that in Figure 1. The isotherms are shifted at low surface pressures to higher areas per molecule compared to Figure 1 due to the high viscosity of the monolayer and the resultant slow relaxation time for the surface pressure. After the first compression (arrow), the cyclic isotherms are very reproducible. (B) Typical isotherm for DPPC/POPG/PA (69/20/11 w/w/w) on water at 37 °C at a compression rate of 0.91 Å^2 mol^{-1} s^{-1}. The cyclic isotherms are very similar to those in (A), especially after the first compression (arrow). No significant variation in the maximum surface pressure, respreading, and monolayer morphology was observed with temperature or compression speed.

hysteresis between expansion and compression cycles are similar under all conditions tested.[11]

Tobacco-Smoke-Exposed Subphases. To determine the effects of exposure to ETS, the lung surfactant lipids were characterized on subphases containing different dilutions of the ETS-exposed stock solution to obtain the equivalent total suspended particulate exposure. Figure 3 shows isotherms of the lipids on subphases with different tobacco smoke exposures at a compression rate of 0.13 Å^2 mol^{-1} s^{-1} to compare to the results of Figure 1 on pure water. The isotherm on the left is on a subphase with an equivalent total suspended particulate exposure of 0.5 mg/m^3, which is similar to the isotherm on pure water (Figure 1). Further compression−expansion cycles lead to partial reversibility. This is accompanied by a stepwise drop in the collapse pressure at a given area per molecule.

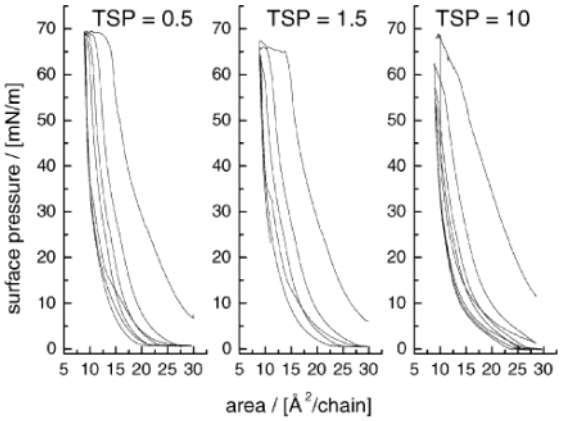

Figure 3. (Left) Model surfactant lipids on a subphase with an equivalent total suspended particulate exposure of 0.5 mg/m^3. Overall, the isotherm is similar to Figure 1, except that the plateau in the isotherm on water at ~18 mN/m (Figure 1) is less pronounced here. The compression rate was 0.13 Å^2 mol^{-1} s^{-1}. Further compression−expansion cycles lead to a stepwise drop in the collapse pressure. (Center) At an equivalent total suspended particulate exposure of 1.5 mg/m^3, a collapse pressure above 65 mN/m can only be obtained in the first two cycles. Subsequent cycles show a steady decrease in the maximum surface pressure. From the shift of the compression cycles to the left, it appears lipid is being lost from the interface. (Right) At a total suspended particulate exposure of 10 mg/m^3, the second cycle already shows a drop in the maximum surface pressure to 62 mN/m and the expansion−compression cycles are no longer reversible.

Increasing the equivalent total suspended particulate exposure to 1.5 mg/m^3 (center) alters the high surface pressure regions of the isotherms dramatically. A collapse pressure above 65 mN/m can only be obtained in the first two cycles. Subsequent cycles show a steady decrease in the maximum surface pressure or minimum surface tension. At an equivalent total suspended particulate exposure of 10 mg/m^3 (right), the second cycle already shows a drop in the maximum surface pressure to 62 mN/m and the expansion−compression cycles are no long reversible. The interaction between the ETS-conditioned subphase and the lipid monolayer has changed how the monolayer collapses (which determines the minimum surface tension) and, apparently, the fraction of surfactant that respreads (which determines the reproducibility of the expansion−compression cycles).[11,52] In addition to the variations at high surface pressures, the increase in ETS exposure also increases the area per molecule at lift-off (where the isotherm first changes from a zero surface pressure), suggestive of some surface activity of the ETS-exposed subphase. This is consistent with the lower surface tension of the ETS-exposed subphase compared to pure water.

Visualizing the monolayers using fluorescence microscopy shows the variation in morphology that accompanies the changes in the isotherms. Figure 4 compares the morphology of the lipid mixture on a pure water subphase (left column) with that of an identical monolayer on a subphase made with an equivalent total suspended particulate exposure of 0.5 mg/m^3 (right column) after the monolayer has been cycled. On water, the lipid mixture exhibits condensed, DPPC/PA-enriched domains (dark) in a continuous liquid-expanded DPPC−POPG matrix (bright)[23,49] at low surface pressures. The fluorescent dye is preferentially excluded from the crystalline DPPC/PA

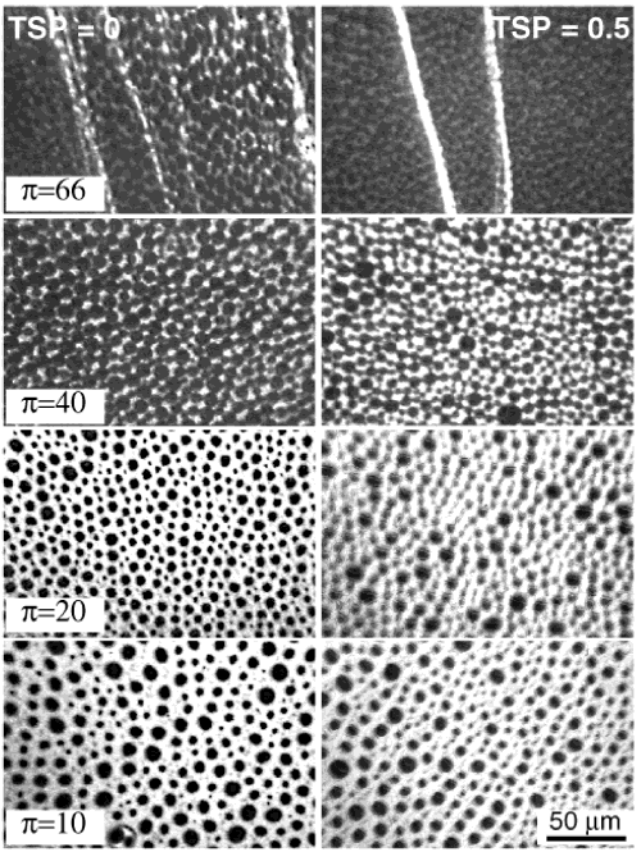

Figure 4. Fluorescence micrographs of the model lung surfactant lipids on pure water (left column) and on a subphase made with an equivalent total suspended particulate exposure of 0.5 mg/m^3 (right column) after cycling. For surface pressures below 40 mN/m, the monolayers have similar morphologies of condensed, DPPC/PA-enriched domains (dark) in a continuous liquid-expanded DPPC−POPG matrix (bright). At 40 mN/m, the monolayer on water (left) is primarily solid phase, with a small fraction of liquid-expanded phase. The monolayer on the tobacco-smoke-exposed subphase (right) is less homogeneously dark, and there is less ordered phase. At the collapse pressure of 66 mN/m, the monolayer on water fractures in multiple locations to form bright cracks from 5 to 10 μm in thickness (top left). For the tobacco-smoke-exposed monolayer, collapse leads to larger cracks with widths of as much as 50 μm. The wider cracks inhibit the reincorporation of the folded regions into the monolayer as they remain in the films even at surface pressures as low as 10 mN/m and lead to the decrease in the maximum surface pressure seen in the isotherms in Figure 2.

domains and concentrated in the more disordered DPPC−POPG phase.[47] The circular domains are between 5 and 15 μm in diameter, and decrease slightly in size as the surface pressure increases. Concurrently, the number of solid-phase domains increases, leading to darker images. At a surface pressure of 40 mN/m, the monolayer consists of homogeneously dark, closely packed solid domains, separated by thin regions of bright liquid-expanded phase. At the collapse pressure of 66 mN/m, the monolayer fractures in multiple locations to form bright "cracks".[18,19,21,22,53] Previous atomic force microscopy observations have shown that these cracks are multilayer patches where the collapsed monolayer folds over onto itself.[18,21,22,54] The material in these folds reincorporates into the monolayer on expansion at pressures below 20 mN/m, which is consistent with the isotherm measure-

(52) Zasadzinski, J. A.; Ding, J.; Warriner, H.; Bringezu, F. *Curr. Opin. Colloid Interface Sci.* **2001**, *6*, 506−513.

(53) Diamant, H.; Witten, T.; Gopal, A.; Lee, K. Y. C. *Europhys. Lett.* **2000**, *52*, 171−177.

(54) von Nahmen, A.; Schenk, M.; Sieber, M.; Amrein, M. *Biophys. J.* **1997**, *72*, 463−469.

ments showing a large expansion in area per molecule between 18 and 10 mN/m.[19] Incorporating the material in the folds into the expanding monolayer leads to a reproducible expansion−compression cycle,[19] but this requires expanding the films to relatively low surface pressures.

On the subphase made with an equivalent total suspended particulate exposure of 0.5 mg/m^3 (Figure 4, right), the morphology at low surface pressures is unchanged. However, at 40 mN/m, the image has a larger percentage of bright, liquid-expanded phase, suggesting a fluidization of the monolayer. It appears that the collapse leads to larger and more varied multilayer folds with an increased width of up to 50 μm. On expansion (*not shown*), the collapsed structures have not completely disappeared at 10 mN/m. On expansion, the monolayer appears more inhomogeneous, suggesting that the more extended folds inhibit the reincorporation of the material in the folds into the monolayer. This is very similar to what was observed for similar monolayers on an albumin-containing subphase.[19] Albumin is known to be an inhibitor of surfactant function.[19]

With increasing ETS exposure, the monolayer morphology is altered significantly. Figure 5 shows the morphology of the condensed monolayers at 40 mN/m during compression (left column) and the collapsed structures at 67 mN/m (right column) at different total suspended particulate exposures. From bottom to top, the equivalent total suspended particulate exposures are 0, 0.5, 1.5, 5.0, 10, and 100 mg/m^3. On water (bottom left), the solid-phase domains (dark) are circular and rather uniform in size, about 10 μm in diameter. At the collapse pressure on pure water (bottom right), multiple, narrow cracks with widths between 5 and 10 μm occur. At 40 mN/m, with increasing ETS exposure, the domain size decreases but the circular domain shape is unchanged. At an equivalent total suspended particulate exposure of 1.5 mg/m^3, the solid domains decreased to about 5 μm in diameter. Concurrently, the width of the collapse structures increased dramatically; at an equivalent total suspended particulate exposure of 5.0 mg/m^3, crack widths were greater than 50 μm. The unfolded regions of the layer lose contrast, and there appears to be no remaining liquid-expanded phase. This suggests a near-complete removal of the POPG and the fluorescent lipid label from the monolayer into the crack structure or into the subphase at high surface pressures. The loss of material to the subphase is consistent with the isotherm measurements (Figure 3), showing a decrease in area after multiple cycles with increasing ETS exposure, which is consistent with a loss of lipids from the monolayer. Monolayers on the subphase with an equivalent total suspended particulate exposure of 100 mg/m^3 showed the most drastic change. The monolayer morphology was inhomogeneous over the entire range of surface pressures, and the bright phases were localized in patches. At collapse, irregular cracks occur where the fluorescent lipid accumulates. Focusing down into the subphase shows that these bright cracks extend micrometers into the subphase, rather than the few bilayer thicknesses in the monolayers on pure water. The unfolded regions of the monolayer are completely dark and without any contrast, suggesting the absence of fluorescence dye and the liquid-expanded phases. Hence, the monolayer on the most concentrated subphases likely only contains DPPC and PA, which are capable of forming solid phases; all of the POPG, which can only form liquid-expanded phases at this temperature,[22] has likely been lost to the subphase and will not respread on subsequent compression−expansion cycles.

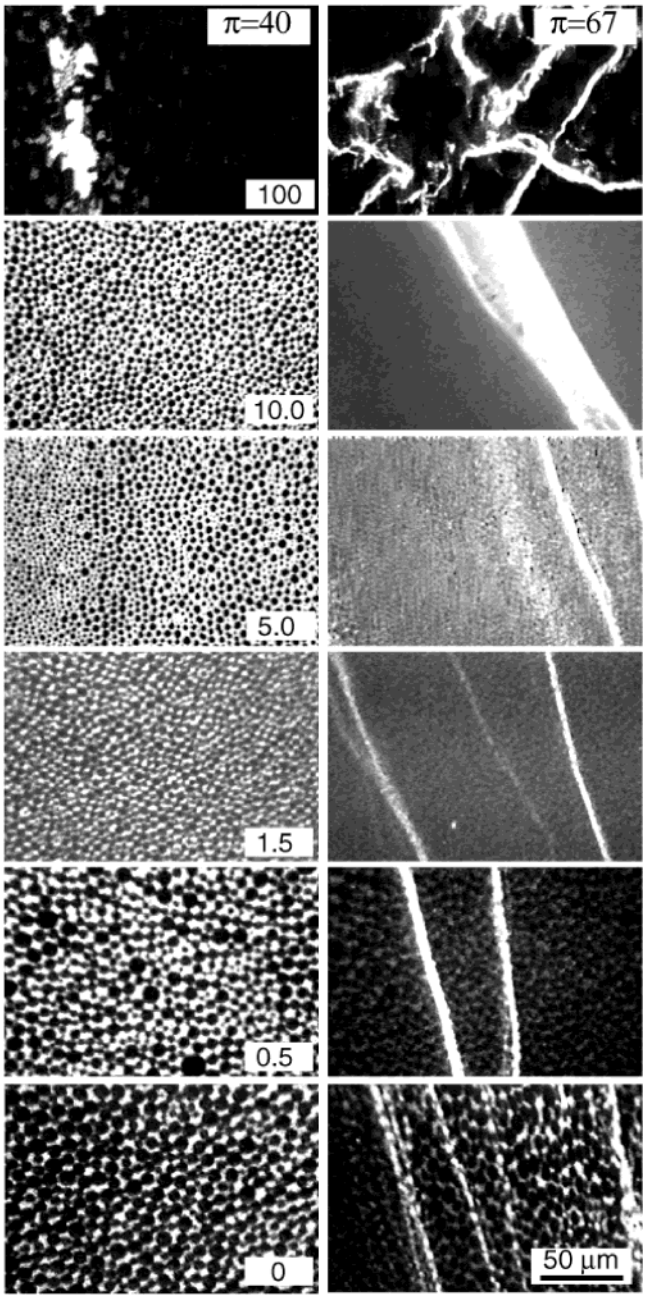

Figure 5. Morphology of the condensed monolayers at 40 mN/m during the first compression (left column) and the collapsed structures at 67 mN/m (right column) at different total suspended particulate exposures. From bottom to top, the equivalent total suspended particulate exposures are 0, 0.5, 1.5, 5.0, 10, and 100 mg/m^3.

To quantify the changes in the monolayer morphology with increasing ETS exposure, a series of low-resolution survey images (not shown) of the monolayers were taken at different surface pressures between 10 and 70 mN/m on subphases with equivalent total suspended particulate exposures of 0, 0.5, and 1.5 mg/m^3 . The images were analyzed by a histogram analysis according to the pixel gray level (Figure 6). A color index of 0 corresponds to black, while a color index of 255 corresponds to white. The comparison is necessarily qualitative rather than quantitative in that the absolute amount of fluorescent dye in a image is not controlled; however, shifts from one end of the index to another are suggestive of changes in the distribution of the fluorescent dye, and hence the distribution of the fluid phases. On pure water, the histogram

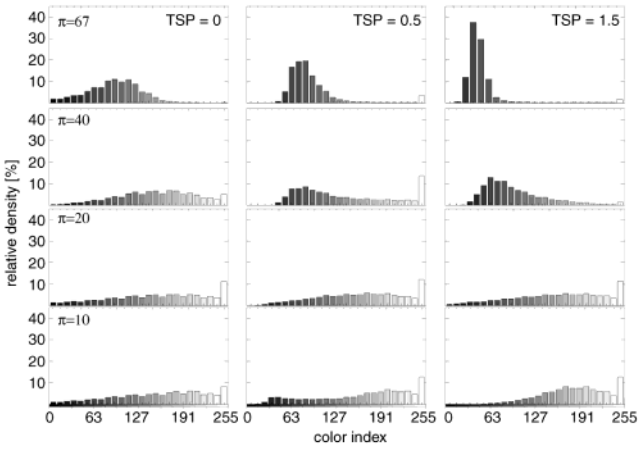

Figure 6. Gray level histogram analysis of low-resolution survey images (not shown) taken at surface pressures between 10 and 70 mN/m on subphases with equivalent total suspended particulate exposures of 0, 0.5, and 1.5 mg/m^3. A color index of 0 corresponds to black, while a color index of 255 corresponds to white. Increasing tobacco exposure leads to a shift in the pixel density toward the black side of the spectrum, implying a loss of fluorescent lipid generally associated with the fluid-phase lipids. At the highest surface pressures investigated, the peak in the pixel gray levels became sharper. This suggests a loss of the liquid-expanded phase common in monolayers, likely due to an elimination of POPG from the monolayer.

shows a homogeneous distribution of gray levels with a slightly higher pixel density at the white end of the spectrum. On subphases exposed to ETS, even at very low levels, a maximum in the gray level distribution occurs. Increasing surface pressure shifts this maximum toward the black side of the spectrum. At a pressure of 40 mN/m, the tobacco-exposed monolayers show a pronounced dark shift of the distribution. This is consistent with a loss of the liquid-expanded phase, and likely a loss of POPG from the monolayers with increasing ETS exposure. There is also a more pronounced spike in the distribution at the maximum of the color index, which also is consistent with more of the fluorescent dye being concentrated in less liquid-expanded phase. At the highest surface pressures investigated, the peak in the pixel gray levels became sharper. At a total suspended particulate exposure of 1.5 mg/m^3 and 70 mN/m surface pressure, more than 90% of the pixels were in the gray range of 1−100, as compared to the more uniform spread from 1 to 255 for the monolayers on pure water. This suggests almost a complete loss of the liquid-expanded phase common in monolayers on pure water.

Discussion

The epithelial lining fluid and lung surfactant are certainly exposed to ETS during normal breathing in a room where smoking occurs. Previous work has shown that damage can occur to lung surfactants with a subsequent loss of performance when exposed to various oxidizers or free radicals.[10,16,17] It would not be surprising to find that the constituents of ETS, which is known to contain both free radicals and strong oxidizers, might chemically or physically alter lung surfactant and impair surfactant function.[1] Our study does not address the variation in lung penetration on the size or chemical reactivity of the constituents of tobacco smoke, or on variations in ETS concentration and the duration of exposure depending on the amount or duration of smoking or ventilation. We used water conditioned by exposure to ETS in a controlled environment as a model of exposing the epithelial lining fluid to the chemicals in ETS. This choice of model system is dictated somewhat by our choice of the Langmuir trough and fluorescence microscopy as the tools to study the surfactant. Of course, only those components of ETS that are soluble in the subphase water can interact with the surfactant in our model system; hence, we are probably underestimating the actual effects of ETS on the surfactant. An alternative solution would be the direct exposure of the interface to tobacco smoke; however, that would lead to particulate matter contaminating the interface which would dominate both the images and the isotherms. Here, we are more concerned with the chemical interactions between those compounds soluble in the liquid layers covering the epithelial lining of the lungs and the lipids in lung surfactant. In future work we plan to use bulk surfactant suspensions that have been exposed for longer times to smoke-conditioned water or saline, and then spread that material on a clean interface.

The lipids used in this study are the primary lipid constituents of the clinically used replacement pulmonary surfactant Survanta.[13] Lung surfactant is responsible for the adjustment of the physicochemical parameters of the alveolar interfaces, especially the surface tension during breathing. Both the isotherms and the fluorescence measurements indicate changes in monolayer phase behavior and morphology on addition of the ETS-conditioned water to the subphase. ETS exposure alters the distribution and fraction of both liquid-expanded and crystalline lipid domains, which previous work has shown influences the minimum surface tension[18,21,23,49] and monolayer viscosity[26] in pristine lung surfactant monolayers. Exposure to ETS removes the unsaturated lipids such as POPG that form a liquid-expanded phase network, which separates the condensed-phase domains on compression. This change affects the collapse structures of the lipid films, leading to higher minimum surface tension. The loss of fluorescence intensity shown in Figure 6 is consistent with the remaining monolayer becoming enriched in DPPC and PA, which both form rigid, condensed films that do not respread well after collapse, due to a loss of fluid-phase POPG. Altering the respreading process of the monolayer leads to poor coverage of the interface, a further loss of material, and subsequently higher minimum surface tensions. The increase in the minimum surface tension and respreading of the monolayer will likely alter the fluid distribution in the alveoli and likely the work of breathing.[11] These results are consistent with the observations of Subramaniam et al., who found that the respreading and compressibility of extracts of BAL from smoke-exposed rats were inferior to those of the controls.[40] However, those authors ascribed these differences to a decrease in the saturated lipid fraction of the BAL extract, while our images show that the monolayers actually have an increased saturated lipid content. These physical and chemical alterations of the breathing process may promote inflammation and edema, further impairing the surfactant system.[10]

Future work will focus on chemical analysis of the monolayers to determine the fate of the unsaturated lipid constituents of lung surfactants that make up the liquid-expanded phases present at collapse in monolayers on pristine subphases, but absent on ETS-exposed subphases. The unsaturated lipids are the most vulnerable to oxidation and chemical degradation by the compounds in ETS. We will also examine the effects of the lung surfactant proteins, especially SP-B[21] and SP-C,[18,54] which modify the collapse structures and make the monolayer easier to respread after collapse. There is some evidence that the

fraction of SP-B in particular is reduced by exposure to tobacco smoke.[41] Fully functional SP-B and SP-C may reduce the damage due to ETS exposure, especially by modifying the collapse and respreading of the lipid monolayers.[18]

Acknowledgment. We thank Dale Uyeminami for assistance in preparing the tobacco-conditioned subphases. F.B. acknowledges financial support from the Deutsche Forschungsgemeinschaft (Emmy-Noether-Program Grant BR 1826/2-1). J.A.Z. acknowledges NIH Grant HL-51177 and University of California TRDRP Grants 8RT-0077 and 11RT-0222. K.E.P. acknowledges University of California TRDRP Grant 7RT-0118.

LA026455E